PROGRESS REPORT
NATIONAL AERONAUTICS AND SPACE ADMINISTRATION
GRANT NAG 5-1129

M. A. Coplan
January 1995

Introduction

In the last six months a major effort has been the organization of work on the composition of solar wind emanating from solar coronal holes. A review for the IUGG summarizing recent solar wind composition research was completed and will appear this year. The manuscript is included at the end of this report.

Data Analysis

Over the last two years a large amount of analysis has been done with solar wind composition from coronal mass ejections and coronal holes. Because a number of different students did the work, the results were in different formats, and it was difficult to apply consistent analysis criteria. We have now organized the data and results from coronal holes and a master list of coronal holes for the years 1978 to 1992 has been prepared. A copy of the list is included at the end of the report.

We have now established a standard procedure for analyzing ICI results and storing the results. For coronal holes the procedure is listed below:

1. Determine the period coronal holes on the sun are in earthward direction using the coronal hole information from Catalogue of Coronal Holes 1970-1991
2. Compute the solar wind sun/earth transit time.
3. Examine helium velocity, density, and temperature (VDT) data for the period of the selected coronal hole, taking into account the solar wind transit time. In the VDT data we look for a solar wind velocity increase accompanied by a density and temperature decrease.
4. For spectra that meet the VDT criteria run PRINT_ICE. This program puts the satellite data in a 7 column format. The data in this format must meet the following criteria:

    a) all 7 columns present.

    b) maximum number of counts in the center column at mass per charge channel 11

    c) maximum count channel each row be in the same column

    d) number of counts at the peak $\leq$ 1500

e) no more than a 3 or 4, -1s in the spectra. -1 is the bad data flag.

Spectra not meeting the above criteria are rejected We regularly use less than 50% of the spectra.

5. The selected spectra are analyzed with one of the following programs,

a) ICWIND_KB

b) JOEY.COM. This program runs ICWIND_KB_JDN in an automated way and takes 20% of the time of ICWIND_KB for a series of spectra. The ICWIND_KB_JDN program has been modified to list the abundance of iron.

6. The programs create 4 output files with the results,

a) Short Form used for analysis.

b) The Long Form, the most comprehensive file.

c) The Print File, obsolete.

d) for036.dat or ion File, used to make the ICI mass/charge graphs.

All files are put into the weekly$ disk in the Goddard computer.

7. The files are copied onto the Maryland computer Godzilla, then down loaded to the Macintosh.

8. The results from the Short Forms are entered into a spreadsheet template for further analysis. From the spreadsheet abundance ratios are plotted, printed and copied to floppy disk. The most recent results are contained in loose-leaf notebooks.

A flow chart of the data analysis procedure is included at the end of the report.

All but 2 coronal holes for 1981 have now been analyzed. The first months of 1980 have been examined for likely coronal holes. Those that have been found fail to meet the VDT criteria. The year of 1982 appears to have been finished but, will be checked for completeness.

A method to modify the analysis program to include the middle three columns is underway.

Solar Wind Composition
from Coronal Holes

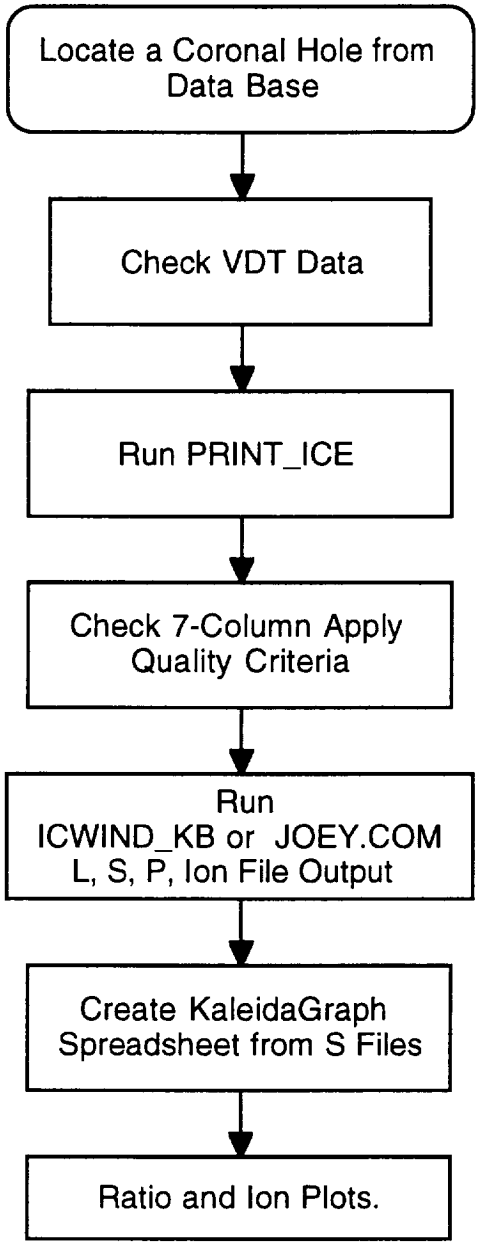

Coronal Holes

Year	Calendar Date	Decimal Day	Latitude Range	Velocity, Density, Temperature Period	Velocity, Density, Temperature Summary	7-Column Period	7-Column Summary	Remarks	Analyzed By
1978									
	1/4/78	3						Pre-Launch	
	3/11-12/78	68-69						Pre-Launch	
	5/5-6/78	124-125						Pre-Launch	
	8/1/78	212						Pre-Launch	
	9/2-3/78	244-245							
	10/23-24/78	295-296							
	12/18-19/78	351-352							
1979									
	2/4/79	34							
	2/22/79	52							
	3/16/79	74		80.0-82.8		80.0-82.8	Bad Data	On File	KB
	4/11-12/79	100-101							
	4/16-17/79	105-106							
	5/8-9/79	127-128		130.07-130.45	Incomplete			Incomplete	KB
	6/3-5/79	153-155							
	6/10-11/79	160-161							
	7/27-28/79	207-208							
	8/22-23/79	233-234							
	12/5/79	338							
1980									
	1/1-2/80	0-1		2-7.	Plot on File				
						20-26	<7 Columns, Several -1s, Skew		
	5/7-8/80	127-128		130-137	Plot on file				
	6/4/80	155		157-166	Plot on file				
	6/29-30/80	180-181			Bad Data			Bad Data	
	7/13/80	194		200-206	Plot on file	297		Not Consistent w/Date	
							ICI Plots in Files, No 7-Column	ICI Plot on File	
	10/27-28/80	300-301	22 N to 50 S			302-307	?	Not Consistent w/Date	
	11/24/80	328			Not in date			Not Consistent w/Date	
	12/21/80	355							
1981									
	1/17/81	16			No data			No Data	
	2/22/81	52		55.2		55.2-58.9	Some Data at Extremes, <1500	Ion Plots 55-58	KB
		91-95	48	92-99	Maybe	92-99	Criteria Not Met		ML
		117-118	10	118-125	Good	118-126	Criteria Not Met		ML
	6/5-7/81	155-157			Many bad pts.			Bad Data	
	7/2-3/81	182-183			Inconsistent			Inconsistent	
		211-212	22	211-220	Good	211-220	Criteria Not Met		ML
	8/11-13/81	222-224	25	222-230	Good	222-228	Criteria Not Met		ML
	8/26/81	237		236-245	Good/Slow	232-244	Good		KY
	9/8/81	250			No good			Bad	
	9/23/81	265.5				266-277	Good, Completed		ML
	10/5/81	277.4				278-285	Good, Completed		ML
		286-287	10	287-295	Good		Criteria Not Met		ML
		320-321	22	320-327	Good	320-327	Criteria Not Met		ML
	12/23/81	356	5 N to 5 S	up to 362				Up to 362	

Coronal Holes

1982								Not Consistent w/Date	
	1/19/82	18	15 N to 7 S	17-26	Plots	21-25	Bad , <1500, Too many -1	Some Ion Plots	KB
	2/15/82	45	8 N to 19 S	46-54		46-47	Good	Some Ion Plots	KB
						51-58	Bad, Skewing		
	2/23-24/82	53-54	6 N to 19 S			56.0-58.9	Analyzed for 57.7, Many Bad Data	Ion Plots 58	KB
	3/14-15/82	72-73	6 N to 22 S	75-80		75-77	<5-columns,<1500, -1	Ion Plots 75	KB
	3/22/82	80	10 N to 10 S					No, day 85 on file	KB
	4/10/82	99	7 N to 4 S					Bad	KB
	4/19/82	108	17 N to 15 S	109.5-111.5	Good	109-114	Completed	Ion Plots109	KB/ML
	4/26-27/82	115-116	17 N to 12 S	118-126				Some Ion and Ratio Plots 120-121	KB
	5/11-17/82	130-139	12 N to 15 S	135-139		133.5-140	Completed	Ion Plots 138	KB/JN
	5/23-24/82	142-143	11 N to 9 S			145-147	Short, Many Bad Data.		KB
	5/26-27/82	145-146	90 N to 4 S	145-154			Group with Above	Ion Plots 145	KB
	6/11/82	161	12 N to 5 S	162-168	Plots			?	KB
	6/19-20/82	169-170	12 N to 10 S			173-177		Dates do not match	KB
	6/21-22/82	171-172	55 N to 2 S	176-183	Plots		Completed		KB/ML
	7/7-8/82	187-188	30 N to 7 S	190-196	Plots		Bad		KB
	11/24/82	327	8 N to 2 S		No Data			No Data	KB
	11/27/82	330	12 N to 8 S	331-336	Plots			No Data	KB
	12/4/82	337	12 N to 8 S	341-346	Plots				KB
1983									
	1/12-14/83	11-13.	5 N to 8 S		No Data			No Data	
	1/20-22/83	19-21	13 N to 11 S		No Data			No Data	
	2/12-13/83	42-43	21 N to 3 S	43-49	Plots			43-49	
	2/16-17/83	46-47	33 N to 17 S						
	3/11-12/83	69-70	12 N to 8 S						
	3/16/83	74	70 N to 12 S						
	3/26/83	84	18 N to 30 S						
	4/4-6/83	93-95	25 N to 32 S						
	4/11-12/83	100-101	70 N to 5 S						
	4/17/83	106	20 N to 6 S						
	4/21-22/83	110-110	18 N to 30 S						
	4/30-2/83	119-121	35 N to 10 S						
	5/10/83	129	70 N to 26 S						
	5/14/83	133	14 N to 7 S						
	5/18-20/83	137-139	12 N to 35 S						
	5/28/83	147	25 N to 25 S						
	6/15/83	165	21 N to 6 S						
	7/28/83	208	70 N to 3 S						
	8/9-10/83	220-221	18 N to 4 S						
	9/28/83	270	5 N to 12 S						
	10/4-5/83	276-277	5 N to 20 S						
	10/31-1/83	303-304	31 N to 25 S						
	11/13/83	316	22 N to 3 S						
	11/21/83	324	4 N to 28 S						
	11/26-28/83	329-331	38 N to 28 S	331-336		333-334			
1989									
	3/1-2/89	59-60	5 N to 11 S	58-72	On Disk			ICI graph on file	
	3/28-29/89	86-87	15 N to 9 S	84-92	On Disk			Bad	
	5/10/89	129	23 N to 3 S						
	5/13/89	132	8 N to 6 S					ICI graphs on file	

Coronal Holes

	5/21-23/89	140-142	50 N to 0	143-148	On Disk				Sanjay
	10/28/89	300	23 N to 11 S	300-310	On Disk				
	10/31-1/89	303-304	12 N to 2 S	Above	On Disk				
	11/28/89	331	11 N to 20 S	332-346	On Disk				Sanjay
	12/4/89	337	25 N to 9 S	Above	On Disk				

SOLAR WIND COMPOSITION

K. W. Ogilvie

Extraterrestrial Physics Branch

Goddard Space Flight Center

Greenbelt, Maryland 20771

M. A. Coplan

Institute for Physical Science and Technology

University of Maryland

College Park Maryland 20742

Abstract

Advances in instrumentation have resulted in the determination of the average abundances of He, C, N, O, Ne, Mg, Si, S, and Fe in the solar wind to approximately 10%. Comparisons with solar energetic particle (SEP) abundances and galactic cosmic ray abundances have revealed many similarities, especially when compared with solar photospheric abundances. It is now well established that fractionation in the corona results in an overabundance (with respect to the photosphere) of elements with first ionization potentials less than 10 eV. These observations have in turn led to the development of fractionation models that are reasonably successful in reproducing the first ionization (FIP) effect.

Under some circumstances it has been possible to relate solar wind observations to particular source regions in the corona. The magnetic topologies of the source regions appear to have a strong influence on the fractionation of elements. Comparisons with spectroscopic data are particularly useful in classifying the different topologies.

Ions produced from interstellar neutral atoms are also found in the solar wind. These ions are picked up by the solar wind after ionization by solar radiation or charge exchange and can be identified by their velocity in the solar wind. The pick-up ions provide most of the pressure in the interplanetary medium at large distances. Interstellar abundances can be derived from the observed fluxes of solar wind pick-up ions.

Introduction

The composition of the solar wind is a tangible measure of the region of the sun from which it originates, the solar corona. The solar wind also sweeps up material from the regions of interplanetary space through which it passes. There are many sources of entrained material including comets, asteroids, the atmospheres of planets and satellites and material from the local interstellar medium. When the entrained material can be distinguished from solar material, solar wind composition measurements provide information on the extrasolar sources. This review is divided into two parts, one dealing with solar wind composition and the sun, the other dealing with some sources of solar wind material other than the sun.

Overall Properties of the Solar Wind and Solar Wind Instrumentation

The solar wind is approximately 95% protons (H^+), 4% alpha particles (He^{++}) and 1% minor ions, of which carbon, nitrogen, oxygen, neon, magnesium, silicon and iron are the most abundant. Solar wind velocity when measured in the ecliptic plane is normally in the range from 300 to 600 km/s, but under some conditions can exceed 1000 km/s. The energy of solar wind ions is from 0.5 to 2.0 keV/nucleon. The density of the solar wind is normally between 1 and 10 particles/cm^3, and the temperature associated with the random motion of the particles is in the range from 10^4 to 10^6 K. A second temperature, referred to as the coronal temperature, is used to characterize the solar wind, it is derived from the relative charge state distributions of the wind elements and is typically of the order of the temperature of the solar corona, 10^6 K (Hundhausen, 1972).

The first space-based composition measurements were of the proton to alpha particle ratio. These measurements used simple electrostatic energy analyzers and relied on the fact that the mean energy per charge of the alpha particles is twice that of the protons (Neugebauer and Snyder 1966). During periods of high density, low velocity and low temperature, minor ion composition can be measured with high resolution electrostatic energy analyzers (Bame et al., 1968), but composition over a wide range of solar wind conditions requires more complex instruments. These instruments are generally of two types, the combined velocity filter-electrostatic energy analyzer and the time-of-flight mass spectrometer. The first instrument measures ion velocity and energy per charge separately. From the two measurements, mass per charge is derived (Coplan et al. 1978). One limitation of this instrument is the need to scan over the full ranges of both velocity and energy per charge. This results in a low duty cycle; a disadvantage that can only be partially overcome with adaptive scanning schemes. A second limitation is overlapping values of mass per charge. For example, alpha particles and C^{+6} have the same mass per charge and cannot be separated with the instrument. As a result, the abundance of C^{+6} can only be inferred from measurements of the other charge states of carbon. This is done by assigning a value of coronal temperature to the solar wind. For cases where the most abundant charge state of an element is obscured, a large uncertainty in the abundance of the element is introduced.

For time-of-flight spectrometers, the energy per charge, velocity and total energy of each ion are determined with a triple coincidence scheme (Gloeckler et al. 1992). With this information, the mass and charge state of each ion are determined. These instruments can cover a wide range of solar wind velocities and have a very low background. The duty cycle for these instruments is determined by the number of energy per charge steps needed to cover the full energy per charge range.

More recently, isochronous time-of-flight instruments have been developed to measure ion mass directly (Möbius et al. 1990, Hamilton et al. 1990). These instruments use electric deflection fields shaped in such a way that the residence time of an ion in the field is inversely proportional to the square root of the mass of the ion, independent of the energy of the ion. For isotope abundance measurements it is necessary to be able to distinguish ions differing in mass by 1 amu for masses as large as 100 amu. This is now possible with these instruments.

Solar Composition

Long term averages. Presently available long term average composition results have mainly been based on the data from the Ion Composition Instrument (ICI) aboard the ISEE-3/ICE spacecraft (Coplan et al. 1978). The instrument is composed of a velocity filter and electrostatic energy analyzer and has produced on average 30 to 50 mass per charge spectra per day with a maximum resolution of 30 since operation began in August, 1978. Average abundance ratios over a complete solar cycle for $^3He/^4He$, $O/^4He$, $Ne/^4He$, $Fe/^4He$, and $Si/^4He$ have been derived from the data. These have been converted to ratios with respect to oxygen and are listed in Table I. The table also contains abundance ratios from other solar wind experiments and solar energetic particle (SEP) (energies of 1 MeV/nucleon) and galactic cosmic rays (energies of 100 to 1000 MeV/nucleon). Also included are abundance ratios for the solar photosphere. The ISEE-3/ICE long term values for the $^3He/^4He$ and Ne/He ratios are in good agreement with ratios determined from foil measurements performed on the lunar surface during three separate Apollo missions. There is also good agreement between the ISEE-3/ICE measurements for oxygen, silicon, and iron and abundances derived from the Solar Wind Ion Composition Spectrometer (SWICS) experiment aboard the Ulysses spacecraft, SEPs, and galactic cosmic rays.

Additional insight into solar wind abundances comes from a comparison of solar wind abundance ratios and solar photospheric abundance ratios as a function of the first ionization potential, Figure 1. Also included are the data for SEPs and galactic cosmic rays (because the spectra of the inert gases are absent in the photosphere it is not possible to compare the solar wind values of ratios of ^{3}He and Ne to ^{4}He to those in the photosphere). There is a systematic difference between the three sets of abundance data and photospheric abundances. Elements with low first ionization potentials (FIPs) are more abundant than high FIP elements (Meyer 1985, Hovestadt 1979). The transition between low and high FIP elements occurs at about 10 eV, corresponding to Lyman-alpha radiation. It appears that atomic physics is much more important in determining abundances in the solar wind, SEPs and galactic cosmic rays than the details of the structure of the stellar atmosphere from which the particles originate and the acceleration mechanisms that are responsible for their final energies. The similarities in composition obtained by the different techniques provides us the possibility of applying knowledge gained from solar wind studies to SEPs and galactic cosmic rays.

Any model of the solar wind must take into account the conditions in the photosphere, chromosphere, and corona, for it is the photosphere that feeds material up through the chromosphere to the corona, and photospheric abundances are the baseline against which solar wind abundances are compared. The photosphere can be adequately described as a gas in thermodynamic equilibrium with a temperature of approximately 6500 K. The corona, by contrast is much less dense with a temperature of the order of 10^6 K so that the assumption of local thermodynamic equilibrium is sometimes questionable. The mechanism of coronal heating is presently not well understood; even within the transition region there are steep temperature and density gradients. Within the corona, the temperature is a minimum at the base where the density is greatest. Farther

up, temperatures increase and densities fall until mean free paths become comparable to 1 AU and the gas is essentially collisionless. The overall result is a dynamic competition as a function of height between collision frequency, charged particle density (ions and electrons), and ionization efficiency. Because the source region for the solar wind is the outer corona, solar wind composition and charge state distributions reflect the complex kinetics within the corona. Moreover, the mechanisms that produce the transition from the relatively cool, dense photosphere to the hot tenuous corona are unknown and constitute one of the important outstanding questions about the sun. While it is well established that ionization first takes place at the base of the corona, the mechanisms by which initially formed ions are preferentially swept upward and incorporated in the solar wind has yet to be fully explained. Current models hypothesize the existence of radial magnetic structures at the base of the corona that confine the ion trajectories to paths that lead into the corona. Neutral atoms, by contrast, are free to diffuse in all directions.

Fractionation in the corona has been modeled by von Steiger and Geiss (1989) who have been able to reproduce a FIP effect of approximately the observed size using fairly simple models of fractionation by ion-atom separation across magnetic field lines in the upper chromosphere. Their mechanism relies upon trapping of charged particles on magnetic field lines. In a constant UV flux, the difference in ionization times between high and low FIP atoms results in the preferential containment of low FIP atoms on magnetic field lines that conduct them up through the corona. This mechanism can reproduce the FIP effect for temperatures of 10^4 K, densities of $\leq 10^{16}$ m^{-3}, and an overall height scale of 10 to 100 km. The theory also predicts a slight decrease in the abundance of He, in agreement with the data in Table I. Burgi (1992), has shown that the flow geometry in coronal streamers can also produce strong helium fractionation, and, in absence of a verified source for the slow solar wind, such geometrical effects could probably produce the variabilities seen at low speeds.

The only isotope measurements currently available are those for the He^3/He^4 ratio (see Table I). A knowledge of this ratio constitutes a stringent test of models of solar evolution (Maeder, 1990).

Solar Wind from Well Defined Solar Structures. In an effort to learn more about the solar FIP effect and thereby gain additional knowledge about the structure and dynamics of the photosphere, chromosphere and corona, scientists have begun to analyze the composition of solar wind that originates from well defined structures on the sun. So far it has been possible to identify solar wind from coronal mass ejections, coronal holes and sector boundary crossings. These structures are associated with different magnetic field topologies that certainly play a central role in the transport and fractionation of ions and electrons from the chromosphere to the corona and solar wind. In addition to direct solar wind measurements, there are now spectroscopic studies of the abundances of a number of elements in solar flares, active regions and polar coronal holes. These spectroscopic measurements are based on data from a variety of imaging spectrographs operating from the ultra violet to x-ray region of the electromagnetic spectrum. Many of the measurements were taken during the Skylab missions, but only recently have been analyzed in detail (Feldman (1992) and references therein). Most of the work has concentrated on the difference in the abundances of low and high FIP elements under different conditions. The elements that have been analyzed are the low FIP elements, Mg, Na, Fe, Ca, and Si. These have been compared with the high FIP elements Ne and O. The solar flare results are particularly interesting because of the connection between coronal mass ejections and flares. Schmelz (1993), Schmelz and Fludra (1994) have analyzed x-ray spectroscopic observations from the Solar Maximum Mission (SMM) spacecraft and derived abundances for O, Ne, Mg, Si, S, Ca, and F for two flares. These abundances show a gradual, rather than abrupt, change as a function of the FIP, when

compared to solar abundances. The magnitude of the FIP effect was approximately two, and there was a negligible change in abundances as a function of time.

Coronal mass ejections (CMEs)

are some of the largest scale physical phenomena observed on the sun. They are thought to arise from closed magnetic field structures rooted in the solar corona. These structures become unstable which results in the expulsion of large volumes of coronal plasma into the interplanetary medium (Sheeley et al. 1985). Subsequent rearrangement of the magnetic field on the sun is thought to lead to flares. There have been a number of studies of the composition of coronal mass ejecta that have been incorporated into the solar wind. Identification of CME material has relied on the observation of helical magnetic field structures in the interplanetary medium (Burlaga et al. 1982) and bi-directional streaming of electrons and solar energetic particles along the field (Gosling et al. 1987). Low temperature and high velocity are other signatures. A difficulty with the solar wind studies is the uncertainty in associating the solar wind material with the mass ejection. This is due to the fact that most satellite based instruments have been located very near the earth-sun line and at this position can only intercept material from regions of the sun directly facing the earth. Optical observations of mass ejections from these regions of the sun are particularly difficult to make because of the absence of contrast between the ejection and the solar background. On the other hand, there is a great wealth of optical data on mass ejections originating from the limbs of the sun where the ejections stand out against the background of interplanetary and interstellar space. The CME project, initiated in 1991, sought to take advantage of the position of the ISEE-3/ICE spacecraft off the west limb of the sun to make the observations of CME material as it passed the spacecraft (Richardson et al., 1994). Using optical and radio data first from the SMM spacecraft and then ground stations it was possible to identify periods when CME material passed the spacecraft . Because of limitations in telemetry, the

observations were incomplete, but there were sufficient data to identify differences between material from CMEs and the average solar wind. Results of CME composition observations are listed in Table II.

Sector boundary crossings are open field structures associated with reversals in magnetic polarity on the surface of the sun. It has been established for some time that the alpha particle to proton ratio decreases dramatically at a sector boundary crossing (Borrini et al. 1981), but there is very little data on minor ion composition. Some preliminary results are listed in Table II.

Coronal holes are another type of structure on the solar surface. These holes are easily identified on synoptic maps of the solar surface; they are associated with open magnetic field configurations, and are known to be the origin of high speed solar wind. Because of the size of the polar coronal holes the high speed solar wind often carries away most of the mass flux and is therefore of great importance. The abundance of alpha particles is remarkably constant in the high speed solar wind, but highly variable in the slow solar wind (Bame et al., 1977). The Charge Energy Mass (CHEM) instrument aboard the AMPTE spacecraft made a number of composition determinations of high speed solar wind that could be associated with coronal holes (Gloecker et al. 1986). The results relied on the fact that high speed solar wind compresses the magnetosphere so that the spacecraft which was normally inside the magnetopause was temporarily in the magnetosheath, where the abundances of multiply charged ions should not differ appreciably from those in the solar wind. From 1978 to 1982 and again after 1985 the ISEE-3/ICE spacecraft was in the solar wind in a position to observe material from equatorial coronal holes. Though between 10 and 50 equatorial coronal holes were observed each year, the Ion Composition Instrument could only acquire meaningful data

when the solar wind velocity was less than 600 km/s. Only a small number of samples met this criterion, and the results are included in Table II.

In Table II we compare the composition of solar wind from open and closed magnetic field structures, with the average solar wind, and the photosphere from Table I. Also included are composition data derived from the Skylab spectroscopic observations that are also associated with well defined magnetic field topologies. There is a clear correlation between the FIP effect and the topologies. This is especially apparent in the spectroscopic data where the Ne/Mg ratio shows a strong dependence on source region magnetic field configuration. These results are in agreement with those of von Steiger et al. (1992) who find that solar wind from cool coronal sources with open magnetic fields is enriched less in C and Mg than that from hotter closed field sources.

To illustrate this further, in Figure. 2 we show a plot of the ratios O/Ne as a function of the Ne/Mg ratio. The nominal values of the ratios for the corona from SEP measurements and for the photosphere are indicated on the graph. The open circles are the spectroscopic values of Feldman and Widing. We see that, as pointed out by Widing and Feldman, the two points describing material associated with flares lie close to the typical photospheric value, while the others cluster about the typical coronal value. The solid circles are results from the ICI, AMPTE, and SWICS mass spectrometers. The ICI average (see Table I) is identified on the figure together with its uncertainty, which represents real variability as well as measurement uncertainty. The ratio of oxygen to neon as determined with SWICS by Geiss et al. (1994) over a 100 day period at coronal temperatures of 10^6 K and $2x10^6$ K are also shown in Figure 2.

Interstellar Pick-Up Ions

One of the most striking and interesting developments in the last few years has been the detection of extra-solar ions picked up by the solar wind and entrained in its flow. These ions result from the ionization in the interplanetary medium of atoms and molecules, whose source is overwhelmingly the local interstellar medium (LISM). Their presence not only allows us to study many aspects of the LISM from the solar system, but it appears that these pickup ions produce the dominant part of the particle pressure in the outer heliosphere. In an examination of pressure balanced structures observed by Voyager 2 near 35 AU, Burlaga et al. (1994), show that the contributions of the magnetic pressure and the pressure due to pickup ions begin to dominate; beyond this distance the pressure of the solar wind ions and electrons becomes negligible. Thus, in the outer part of the heliosphere, near its interface with the interstellar medium, pickup ions must be of great importance in establishing the location and structure of this interface.

The first observations of interstellar pickup ions (He^+) in the solar wind were made by Möbius et al. (1985), and were explained in terms of an earlier theory developed for the scattering of Lyman alpha radiation from interstellar neutrals. Largely because neutrals are subjected only to gravitational force and radiation pressure, their trajectories can be calculated and their densities in the heliosphere determined. After ionization, the particles gyrate at the solar wind velocity about the magnetic field, with their guiding center moving at the solar wind velocity. The ions form a ring velocity distribution, which pitch angle scattering deforms into a spherical shell. As they move outward from the sun with the solar wind they undergo adiabatic cooling, which reduces the radius of the shell, but they do not become completely incorporated into the solar wind. The velocity distribution function f(v) for pickup ions has been derived by Vasyliunas and Siscoe (1976) in the solar wind frame. A sharp discontinuity in the distribution function

observed in the spacecraft frame at a velocity of twice that of the solar wind is a clear signature of pickup ions even in the presence of another distribution.

Pickup ions are predominantly singly charged, with a small amount of He^{++} being formed by charge exchange with He^{++} in the solar wind. Subsequent interactions of these ions with, for example, propagating or co-rotating interplanetary shocks, further accelerates the ions, and observation of the results of this process may perhaps be used to check models of shock acceleration. Protons and alpha particles from the solar wind are much less efficiently accelerated than He^{+} pickup ions (Gloeckler and Geiss 1994), which strengthens the identification of pickup ions as the source of (usually singly charged) anomalous cosmic rays. Particle acceleration by shocks is, of course, a ubiquitous and important process in this and other galaxies.

The measurement and analysis of pickup ions has been made possible by the development of low background of time-of-flight instrumentation, which uses double and triple coincidence techniques. Because the flux of pickup ions, especially protons, increases with distance from the sun, while that of the solar wind falls, observations at heliocentric distances of several AU are well suited to pickup studies. Recently, Gloeckler and Geiss (1993) have reported measurements of the pick-up ions H^{+}, He^{+}, He^{++}, N^{+}, O^{+}, and Ne^{+} obtained during the Ulysses cruise to Jupiter. They have shown that abundances of these species in the interstellar medium can be deduced from the measurements, and that this method can also be extended to isotopic abundances. This is discussed in detail in Gloeckler and Geiss (1994) and some resulting abundances are shown in Table III. Because interstellar matter is partly in form of grains and may be partly ionized, these abundances are lower limits, which probably explains the quite large differences from solar system abundances, also shown in Table III. In particular, the He/H ratio might have to be amended to reflect better knowledge of the production rate of

He^+. Clearly, however, the measurement of pickup ions can provide useful new information on the constitution of the local interstellar medium.

Finally, we should note that neutrals from planets and comets are ionized and picked up by the solar wind. Although solar system bodies form quite strong local sources - especially comets such as Halley - the LISM is the largest source, and probably the only one which can affect the structure of the heliosphere (Ogilvie et al. 1994, Luhmann 1994).

Conclusions

For several ions that can be separated in mass/charge by an instrument with a resolution of 30, average abundances are now known . Some abundances requiring separate mass and charge separation are also known, and the accuracy of these determinations is approximately 10%, see Table I. This work is still in progress.

Ions with first ionization potentials less than 10 eV are overabundant by as much as a factor of 4 in the solar wind with respect to their abundances in the photosphere. This can be explained by preferential confinement in the local magnetic field moving with the protons. The magnitude of this FIP effect varies with the type of flow. The effect is smaller for flow from coronal holes than from active regions.

Solar wind abundances appear to vary depending upon the magnetic topology of the source region. This aspect of solar wind studies may point a way to the solution to the outstanding question of the origin of the slow solar wind.

With new instruments it will be possible to resolve major isotopes beyond ^3He and ^4He and thus expand studies of the isotopic constitution of the solar corona. From studies of the $^3He/^4He$ ratio it appears that the outer convection zone of the sun is well mixed. More extensive measurements of the isotopic composition promise to provide isotopic ratios for the sun as a body.

The pickup ions, derived from neutral atoms from the local interstellar medium, can be distinguished and measured in the solar wind beyond 1 A.U., making it possible to measure abundances in the LISM using a spacecraft in the locality of the earth. The dynamic characteristics of these ions profoundly affects the outer regions and termination of the heliosphere.

These advances show the that composition measurements in the solar wind are likely to be increasingly useful and rewarding for some time to come.

Acknowledgements

The authors appreciate the help and advice of G. Gloeckler, D. Reames, A. Lukasiak, and P. Bochsler. NASA has contributed to the support of this work under Grant NAG-5-1129.

Ferrando, P., "Cosmic ray propagation and origin", *Proceedings of the XXIII International Cosmic Ray Conference*, Invited, Rapporteur and Highlight Papers, Calgary, Alberta, Canada, 19-30 July 1993, D. A. Leahy, R. B. Hicks, and D. Venkatesan, eds., World Scientific, 1994, pp. 279-306.

Galvin, A. B., G. Gloeckler, F. M. Ipavich, C. M. Shafer, J. Geiss, and K. Ogilvie, "Solar wind composition measurements by the Ulysses SWICS experiment during transient solar wind flows", *Adv. Space Res.* **13**, 75 (1993).

Geiss, J., F. Buhler, P. Eberhardt, C. Filleux, *Apollo 16 Preliminary Science Report*, NASA **SP-315** (1972).

Geiss, J., R. von Steiger, G. Gloeckler, A. B. Galvin, "The neon abundances in the solar wind measured by SWICS on Ulysses"' *EOS* **75**, 278 (1994).

Gloeckler G. and J. Geiss, "Observations of interstellar pickup ions", *Cosmic Winds and the Heliosphere*, in press, (1993).

Gloeckler, G. and J. Geiss, "The abundances of elements and isotopes in the solar wind", *AIP Conference Proceedings* **183**, Cosmic Abundance of Matter, C. J. Waddington, ed., AIP, New York, (1989), pp. 49-71.

Gloeckler, G., F. Ipavich, D. Hamilton, B. Wilken, W. Studemann, G. Kremser, "Solar wind carbon, nitrogen, and oxygen abundances measured in the earth's magnetosheath with AMPTE/CCE", *Geophys. Res. Lett.* **13**, 793 (1986).

Gloeckler, G., J. Geiss, H. Balsiger, P. Bedini, J. C. Cain, J. Fischer, L. A. Fisk, A. B. Galvin, F. Gliem, D. C. Hamilton, J. V. Hollweg, F. M. Ipavich, R. Joss, S. Livi, R. Lundgren, U. Mall, J. F. McKenzie, K. W. Ogilvie, F. Ottens, W. Rieck, E. O. Tums, R. von Steiger, W. Weiss, and B. Wilken, "The solar wind ion composition spectrometer", *Astron. Astrophys. Suppl. Ser.* **92**, 267 (1992).

Gosling, J. T., D. N. Baker, S. J. Bame, W. C. Feldman, R. D. Zwickl, "Bi-directional solar wind electron heat flux events", *J. Geophys. Res.* **92**, 8519 (1987).

Hamilton, D., G. Gloeckler, F. Ipavich, R. Lundgren, R. Sheldon, "New high-resolution electrostatic ion mass analyzer using time of flight", *Rev. Sci. Instrum.* **61**, 3104 (1990).

Hovestadt, D. "Nuclear composition of solar cosmic rays", in *Solar Wind III*, C. T. Russell, ed., Institute of Geophys. and Planetary Phys., University of California, Los Angeles, 1979, pp. 2-5.

Hundhausen, A. J., *Coronal Expansion and Solar Wind*, Springer Verlag, NY, 1972.

Ipavich, F. M., A. B. Galvin, J. Geiss, K. W. Ogilvie and F. Gliem, "Solar wind iron and oxygen charge states and relative abundances measured by SWICS on Ulysses", *Solar Wind Seven*, Proceedings of the 3rd COSPAR Colloqium held in Goslar, Germany, 16-20 September 1991, COSPAR Colloquia Series, Volume 3, E. Marsch and R. Schwenn, eds., Pergamon, 1992, pp. 369-373.

Luhmann, J. G., "Oxygen in the heliosphere", J. Geophys. Res. in press, (1994).

Maeder, A., "A look on non-standard solar models", *Inside the sun*, Berthomieu and Cribier, eds., Kluwer, Dordrecht, (1990), pp. 133.

Meyer, J. P., "The baseline composition of solar energetic particles", *Astrophys. J. Suppl. Ser.* **57**, 151 (1985)

Mobius, E., D. Hovestadt, B. Klecker, M. Scholer, G. Gloeckler, F. Ipavich, "Direct observation of He^+ pick-up ions of interstellar origin in the solar wind", *Nature* **318**, 426 (1985).

Möbius, E., P. Bochsler, A. G. Ghielmetti, D Hamilton, "High mass resolution isochronous time-of-flight spectrograph for three-dimensional space plasma measurements", *Rev. Sci. Instrum.* **61**, 3609 (1990).

Neugebauer, M. and C. W. Snyder, "Mariner 2 observations of the solar wind", *J. Geophys. Res.* **71**, 4469 (1966).

Ogilvie, K. W., G. Gloeckler and J. Geiss, "Neutral oxygen near Jupiter", *Astron. Astrophys.*, in press (1994).

Ogilvie, K. W., M. A. Coplan, J. Geiss, "Solar wind composition from sector boundary crossings and coronal mass ejections", *Solar Wind Seven*, Proceedings of the 3rd COSPAR Colloqium held in Goslar, Germany, 16-20 September 1991, COSPAR Colloquia Series, Volume 3, E. Marsch and R. Schwenn, eds., Pergamon, 1992, pp. 379-384.

Ogilvie, K. W., M. A. Coplan, P. Bochsler, J. Geiss, "Solar wind observations with the ion composition instrument aboard the ISCC-3/ICE spacecraft", *Solar Phys.* **124** , 167 (1989).

Reames, D. V., "Energetic particle observations and the abundances of elements in the solar corona", *Proceedings of the First SOHO Workshop, Annapolis, Maryland, USA, 25-28 August 1992* (ESA SP-348, November 1992), pp. 315.

Richardson, I. G., C. J. Farrugia, D. Winterhalter, "Solar activity and coronal mass ejections on the western hemisphere of the sun in mid-August 1989: association with interplanetary observations at the ICE and IMP 8 spacecraft", *J. Geophys. Res.* **99**, 2513 (1994).

Schmelz, J. T. and A. Fludra, "Absolute abundances of flaring coronal plasma derived from SMM spectral observations", *EOS* **75**, 290 (1994)

Schmelz, J. T., "Elemental Abundances of flaring solar plasma: enhanced neon and sulfur", *Astrophys. J.* **408**, 373 (1993).

Schmid, J., P. Bochsler, and J. Geiss, "Abundance of iron ions in the solar wind", *Astrophys. J.* **329**, 956 (1988).

Shafer, C. M., G. Gloeckler, A. B. Galvin, F. M. Ipavich, J. Geiss, R. von Steiger, K. Ogilvie, "Sulfur abundances in the solar wind measured by SWICS on Ulysses", *Adv. Space Res.* **13**, 79 (1993).

Sheeley, N. R., T. A. Howard, M. J. Koomen, D. J. Michels, R. Schwenn, K. -H. Mulhauser, H. Rosenbauer, "Coronal mass ejections and interplanetary shocks", *J. Geophys. Res.* **90**, 163 (1985).

Vasyliunas, V. M. and G. Sisco, "On the flux and the energy spectrum of interstellar ions in the solar system", *J. Geophys. Res.* **81**, 1247 (1976).

von Steiger, R. and J. Geiss, "Supply of fractionated gases to the corona", *Astron. Astrophys.* **225,** 222 (1989).

von Steiger, R., J. Geiss, G. Gloeckler, H. Balsiger, A. B. Galvin, U. Mall, B. Wilken, "Mg, C, O abundances in different solar wind flow types", *Solar Wind Seven*, Proceedings of the 3rd COSPAR Colloqium held in Goslar, Germany, 16-20 September 1991, COSPAR Colloquia Series, Volume 3, E. Marsch and R. Schwenn, eds., Pergamon, 1992, pp. 399-403.

Widing, K. G. and U. Feldman, "Abundance ratios of oxygen, neon, and magnesium in solar active regions and flares: the FIP effect", submitted to *Astrophys. J.* (1994).

Widing, K. G., U. Feldman, A. K. Bhatia, "The extreme-ultraviolet spectrum (300 - 630 Å) of an erupting prominence observed from Skylab", *Astrophys. J.* **308**, 982 (1986).

Widing, K. G. and U. Feldman, "Abundance variations in the outer solar atmosphere observed in Skylab spectroheliograms", *Astrophys. J.* **344**, 1046 (1989).

Table I
Average Abundances

Element	FIP (eV)	Photosphere[1]	ICI[2] (Average Solar Wind)	SWICS	Lunar Foils[13] (Average Solar Wind)	SEP[14]	Galactic Cosmic Rays[15]
H	13.6	1175±118	-	-	-	1170±90	-
^{4}He	24.6	115±9	75±20[3]	-	75	55±3	-
^{3}He	24.6	-	0.037±0.0004[4]	-	0.032±0.003	-	-
C	11.3	0.43±0.04	-	0.62±0.10[8]	-	0.47±0.014	0.81±0.08
N	14.5	0.132±0.013	-	-	-	0.128±0.004	.049±0.018
O	13.6	1	1	1	1	1	1
Ne	21.6	0.144±0.038	0.17±0.02[5]	0.10-0.12[9]	0.139	0.151±0.005	0.11±0.02
Mg	7.6	0.045±±0.005	-	0.13±0.02[8]	-	0.203±0.008	0.19±0.01
Si	8.2	0.042±0.005	0.12±0.04[6]	0.18±0.02[10]	-	0.155±0.007	0.19±0.01
S	10.4	0.019±0.003	-	0.016±0.007[11]	-	0.036±0.001	0.022±0.003
Ar	15.8	0.004±0.001	-	-	0.004±0.001	0.0033±0.0005	0.0043±0.0016
Fe	7.9	0.055±0.004	0.19±0.01[7]	0.12±0.014[12]	-	0.155±0.015	0.28±0.01

1. Anders and Grevesse (1989)
2. Ogilvie et al. (1989)
3. Bochsler et al. (1985)
4. Coplan et al. (1984)
5. Bochsler et al. (1986)
6. Bochsler et al. (1989)
7. Schmidt et al. (1988)
8. von Steiger et al. (1992)
9. Geiss et al. (1994)
10. Galvin et al. (1993)
11. Shafer et al. (1993)
12. Ipavich et al. (1992)
13. Geiss et al. (1972)
14. Reames (1992)
15. Ferrando (1994)

Table II
Abundances From Various Solar Structures

			ICI[2]			AMPTE[3]	SEP[4]	Skylab Spectroscopy		SMM[7] Spectroscopy
Element	FIP (eV)	Photosphere[1]	CME	SBC	Coronal Hole	Coronal Hole	CIR** Events	Polar Coronal Hole[5]	Flares Active Regions[6]	Flares
H	13.6	1175±118	-	-	-	-	1810±120	-	-	-
^{4}He	24.6	115±9	52	65	48	45±5	159±10	-	-	-
^{3}He	24.6	-	-	-	-	-	-	-	-	-
C	11.3	0.43±0.04	***	***	****	0.53±0.013	0.89±0.036	-	-	-
N	14.5	0.132±0.013	-	-	-	-	0.14±0.014	-	-	-
O	13.6	1	1	1	1	1	1	1	1	1
Ne	21.6	0.144±0.038	0.28	0.17	0.14	-	0.17±0.016	0.14*	0.13-0.21	0.14, 0.32
Mg	7.6	0.045±±0.005	0.12	0.22	0.08	0.106±0.01	0.14±0.014	0.090-0.11*	0.079-0.54	0.20, 0.21
Si	8.2	0.042±0.005	0.10	0.09	0.05	0.103±0.011	0.10±0.012	-	-	0.16, 0.14
S	10.4	0.019±0.003	-	-	-	0.032±0.009	0.05±0.008	-	-	0.036, 0.044
Ar	15.8	0.004±0.001	-	-	-	-	-	-	-	-
Fe	7.9	0.055±0.004	-	-	-	0.124±0.004	0.097±0.011	-	-	0.156, 0.139

1. Anders and Grevesse (1989)
2. Ogilvie et al. (1992)
3. Gloeckler et al. (1986)
4. Reames (1992)
5. Feldman and Widing (1993)
6. Widing and Feldman (1994)
7. Schmelz (1993)

* Based on the assumed value of Ne/O of 0.14
** Corotating Interaction Regions
*** Constrained to 0.45
**** Constrained to 0.55

Table III
Abundances of Pickup Ions at 5 AU Relative to He^+
Data from Gloeckler and Geiss (1994)

Element	Pickup Ion Flux	Interstellar Abundances	Solar System Abundances
H	0.8±0.2	6.2±0.7	10.3
He	1	1	1
C	$\leq 0.4 \times 10^{-3}$	$\leq 0.8 \times 10^{-3}$	$\leq 3.7 \times 10^{-3}$
N	0.8×10^{-3}	0.5×10^{-3}	1.1×10^{-3}
O	5.7×10^{-3}	3.5×10^{-3}	8.8×10^{-3}
Ne	1.2×10^{-3}	1.0×10^{-3}	1.2×10^{-3}

Figure Captions

Figure 1. Solar Wind Relative Abundances to Photospheric Abundances as a Function of First Ionization Potential (FIP). Note that the variability for elements with FIPs less than 10 eV is significantly larger than that for the higher FIP elements. The AMPTE data that are for coronal hole flows show a smaller overabundance below 10 eV than the other measurements.

Figure 2. O/Ne as a function of Ne/Mg for a variety of coronal structures. Neon and magnesium are chosen because they are representative of high and low FIP elements. The open circles are spectroscopic determinations for various structures and events in the photosphere. Determinations from SWICS, AMPTE, and the ICI are also shown. There is a good deal of scatter in the data, however the individual determinations tend to cluster about either the photosphere or coronal (SEP) values. References for the data shown are given below. The following abreviations have been used: "SBC" for Sector Boundary Crossing, "Cloud" for Magnetic Cloud, "CME" for Coronal Mass Ejection and "BDS" for Bi-Directional Streaming Events.

Structure	Instrument	Reference
Solar Wind	SWICS	Geiss et al. (1994)
Open Field	Skylab Spectroscopy	Widing and Feldman (1994)
Prominence	Skylab Spectroscopy	Widing et al. (1986), id. (1989)
Coronal Hole	AMPTE	Gloeckler et al. (1986)
Photosphere	Spectroscopy	Anders and Grevesse (1989)
Corona	SEP	Reames (1992)
Impulsive Flare	Skylab Spectroscopy	Feldman and Widing (1990)
Post Flare Limb	Skylab Spectroscopy	Widing and Feldman (1994)
SBC, Cloud, CME, BDS	ICI	Ogilvie et al. (1992)
ICI Average	ICI	Coplan et al. (1990)
Limb Active Regions	Skylab Spectroscopy	Widing and Feldman (1994), id. (1989)
Flare Decays	Skylab Spectroscopy	Widing and Feldman (1994), id. (1989)

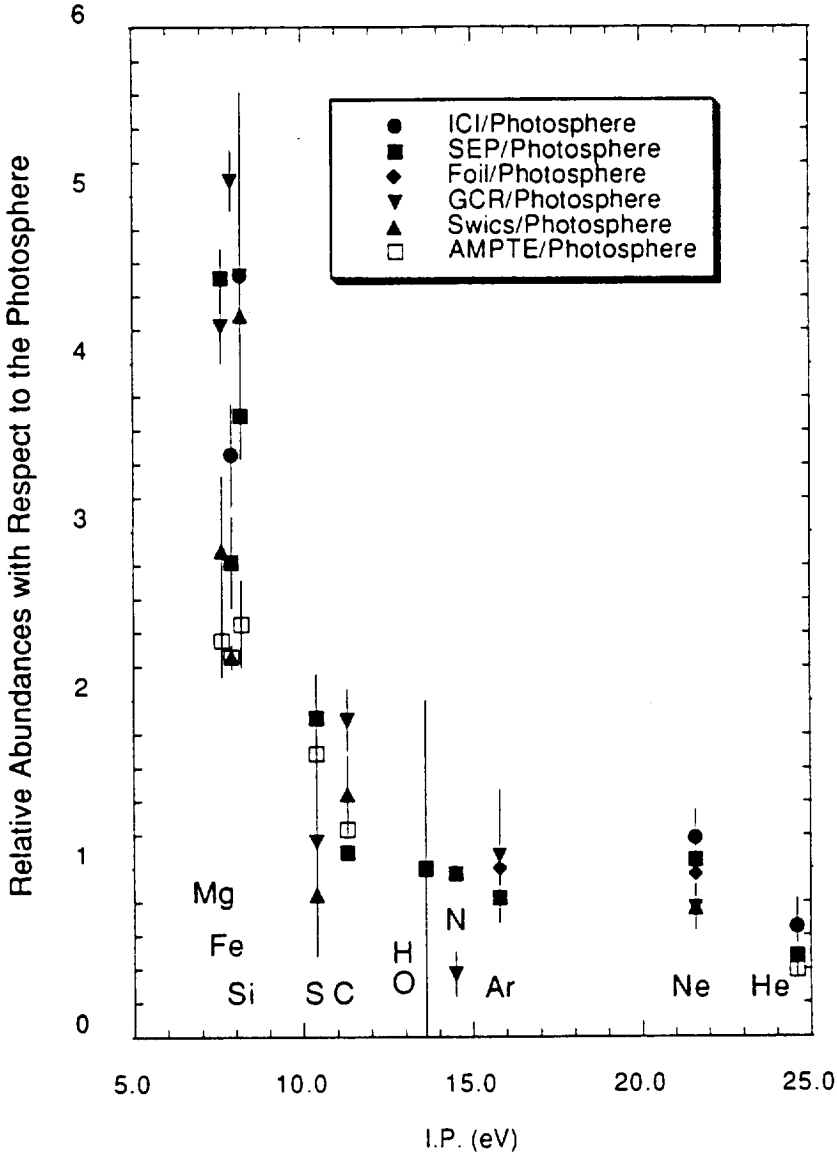
ICI/Photosphere
SEP/Photosphere
Foil/Photosphere
GCR/Photosphere
Swics/Photosphere
AMPTE/Photosphere
Relative Abundances with Respect to the Photosphere
I.P. (eV)
0
1
2
3
4
5
6
5.0
10.0
15.0
20.0
25.0
Mg
Fe
Si
S
C
H
O
N
Ar
Ne
He

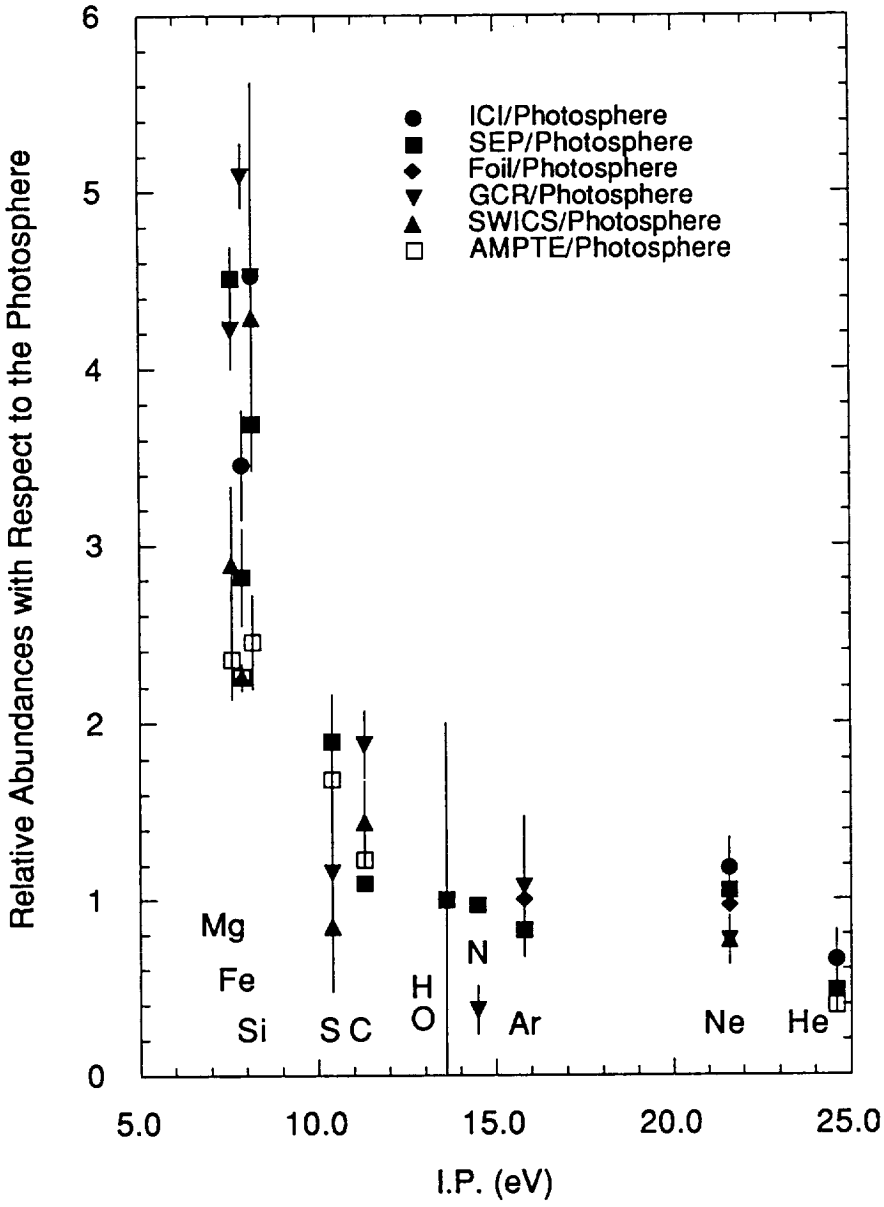
Relative Abundances with Respect to the Photosphere
I.P. (eV)
ICI/Photosphere
SEP/Photosphere
Foil/Photosphere
GCR/Photosphere
SWICS/Photosphere
AMPTE/Photosphere
Mg
Fe
Si
S
C
H
O
N
Ar
Ne
He
0
1
2
3
4
5
6
5.0
10.0
15.0
20.0
25.0

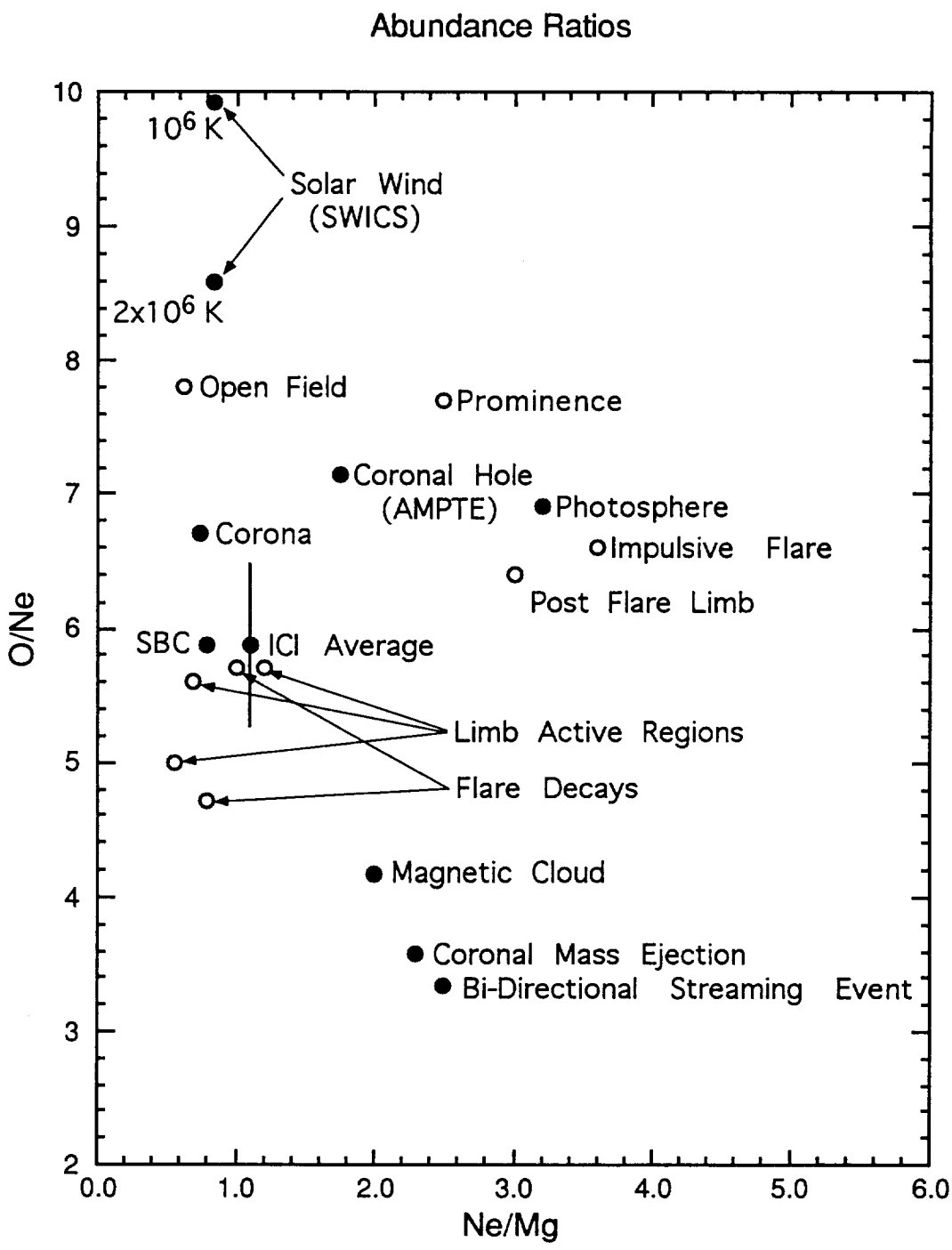
Abundance Ratios
10
9
8
7
6
5
4
3
2
O/Ne
0.0
1.0
2.0
3.0
4.0
5.0
6.0
Ne/Mg
10^6 K
Solar Wind
(SWICS)
2x10^6 K
Open Field
Prominence
Coronal Hole
(AMPTE)
Photosphere
Corona
Impulsive Flare
Post Flare Limb
SBC
ICI Average
Limb Active Regions
Flare Decays
Magnetic Cloud
Coronal Mass Ejection
Bi-Directional Streaming Event